Structural characteristics of isoxazol-3-ol and isothiazol-3-ol, carboxy group bioisosteres examined by X-ray crystallography and *ab initio* calculations

Karla Frydenvang,* Lisa Matzen, Per-Ola Norrby, Frank A. Sløk, Tommy Liljefors, Povl Krogsgaard-Larsen and Jerzy W. Jaroszewski

PharmaBiotec Research Center, Department of Medicinal Chemistry, Royal Danish School of Pharmacy, Universitetsparken 2, DK-2100 Copenhagen, Denmark

Low-temperature single-crystal structure determinations have been carried out on isoxazol-3-ol, 5-methylisoxazol-3-ol, isothiazol-3-ol and 5-methylisothiazol-3-ol, the heterocyclic ring systems used as carboxy group bioisosteres in numerous neuroactive analogues of 4-aminobutyric acid (GABA) and glutamic acid. All compounds form hydrogen-bonded dimers in the solid state. The OH · · · N hydrogen bonds are shorter in isoxazol-3-ols than in isothiazol-3-ols. The excess molecular van der Waals volume of the sulfur-containing ring systems as compared to the corresponding isoxazol-3-ols amounts to about 15%. The sulfur substitution significantly affects the position of the 5-substituents in relation to the heterocyclic ring. Such effects may contribute to the observed differences in pharmacological effects of the structurally related isoxazol-3-ol and isothiazol-3-ol amino acids. The geometries of the compounds have been optimized by *ab initio* calculations at the HF/6-31G* level, and in some cases also at the MP2/6-311G level. The gas-phase calculations are in agreement with the experimental data, especially when correction for the effects of hydrogen bonding is made, as estimated using a complex between isoxazol-3-ol and formic acid. Calculated dipole moments of isoxazol-3-ols and isothiazol-3-ols are similar. Isoxazol-3-ol is more acidic than isothiazol-3-ol by 1.7 pK_a unit as determined by ^{13}C NMR titration, and the differences in acidity are believed to be one of the major factors causing the differences in the biological actions of isoxazol-3-ol amino acids and the corresponding isothiazol-3-ol analogues.**

Introduction

Bioisosteric substitution of the carboxy group is an important approach in the development of selective neurotransmitter receptor ligands. The major central inhibitory and excitatory neurotransmitters, 4-aminobutyric acid (**1**, GABA) and glutamic acid (**2**, Glu), are conformationally flexible molecules, capable of adopting receptor subtype-specific conformations. A number of conformationally restricted analogues of GABA and Glu, in which isoxazol-3-ol (**3**) or isothiazol-3-ol (**4**) units are substituted for carboxy groups, have been synthesized and pharmacologically characterized.[1,2]

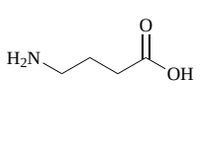

1 (GABA)

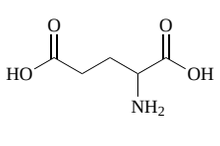

2 (Glu)

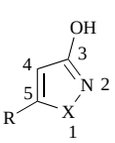

3 X = O, R = H
4 X = S, R = H
5 X = O, R = CH_3
6 X = S, R = CH_3
7 X = O, R = CH_2NH_2
8 X = S, R = CH_2NH_2

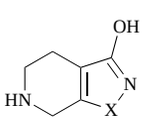

9 X = O
10 X = S

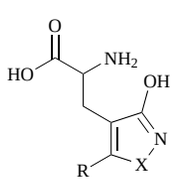

11 X = O, R = CH_3
12 X = S, R = CH_3
13 X = O, R = $C(CH_3)_3$
14 X = S, R = $C(CH_3)_3$

The naturally occurring muscimol (**7**) and the synthetic analogue 4,5,6,7-tetrahydroisoxazolo[5,4-*c*]pyridin-3-ol (**9**, THIP) are $GABA_A$ receptor agonists.[3,4] The two isothiazol-3-ol analogues thiomuscimol (**8**) and 4,5,6,7-tetrahydroisothiazolo-[5,4-*c*]pyridin-3-ol (**10**, thio-THIP) also interact selectively at the $GABA_A$ receptor sites. Thiomuscimol (**8**) is slightly weaker than the corresponding isoxazole derivative **7** as a $GABA_A$ receptor agonist,[5] whereas thio-THIP (**10**) is a competitive $GABA_A$ receptor antagonist.[6]

Using isoxazol-3-ol as the ω-acidic group, a number of subtype-selective Glu receptor ligands has been synthesized, including the two AMPA receptor agonists, (*RS*)-2-amino-3-(3-hydroxy-5-methylisoxazol-4-yl)propionic acid (**11**, AMPA)[7] and (*RS*)-2-amino-3-(5-*tert*-butyl-3-hydroxyisoxazol-4-yl)propionic acid (**13**, ATPA).[8] The corresponding isothiazol-3-ol analogues **12** and **14** have recently been synthesized, and were shown to be selective AMPA receptor agonists.[9] Thio-AMPA (**12**) turned out to be a weaker agonist than AMPA (**11**), whereas thio-ATPA (**14**) was found to be more potent than ATPA (**13**).

These structure–activity relationships demonstrate that the replacement of the isoxazol-3-ol unit with a isothiazol-3-ol unit in neurotransmitter analogues leads to changes in receptor affinity and activity, but in a complex manner. The factors expected to contribute to the differences in the biological effects of isoxazol-3-ol and isothiazol-3-ol zwitterions and amino acids are steric and electronic dissimilarities, as well as differences in acidity and in tautomeric equilibria. No systematic comparison between the structural and physico-chemical properties of these heterocyclic units in a biological context has yet been carried out. In this work, we have compared the structural characteristics of the isoxazol-3-ols **3** and **5** with those of the isothiazol-3-ols **4** and **6**, using X-ray crystallography and *ab initio* quantum chemical calculations. The differences in acidity between the oxygen and sulfur containing heterocyclic units

Table 1 Crystal data, data processing and structure refinement of **3**–**6**[a]

	3	**5**	**4**	**6**
Molecular formula	$C_3H_3NO_2$	$C_4H_5NO_2$	C_3H_3NOS	C_4H_5NOS
Molecular weight	85.0	99.1	101.1	115.2
Crystal size/mm	0.10 × 0.22 × 0.23	0.22 × 0.28 × 0.34	0.02 × 0.12 × 0.46	0.11 × 0.20 × 0.24
Mp/°C	98–99	84–85	71	94–95
Unit cell refined				
No., θ/°	20, 40.40–47.58	20, 37.43–42.85	20, 39.08–42.91	20, 38.31–46.40
a/Å	6.2611(9)	4.640(1)	13.681(2)	6.842(1)
b/Å	8.011(1)	10.134(2)	4.8884(7)	6.861(1)
c/Å	7.086(1)	9.721(2)	13.776(2)	7.373(1)
α/°	90.0	90.0	90.0	100.08(2)
β/°	90.72(1)	93.56(2)	118.41(1)	116.57(1)
γ/°	90.0	90.0	90.0	110.94(2)
V/Å^3	355.39(9)	456.2(2)	810.3(2)	264.9(1)
D_c/Mg m^{-3}	1.590	1.443	1.658	1.444
F(000)	176	208	416	120
Space group	$P2_1/c$	$P2_1/n$	$P2_1/n$	$P\bar{1}$
Z	4	4	8	2
Cu-Kα (λ = 1.5418 Å)	Ni-filter	Gr monochrom.	Ni-filter	Gr monochrom.
hkl-Range	$-7 < h < 4$ $-10 < k < 10$ $-8 < l < 8$	$-5 < h < 2$ $-12 < k < 12$ $-12 < l < 12$	$-17 < h < 14$ $-6 < k < 6$ $-16 < l < 17$	$-8 < h < 5$ $-8 < k < 8$ $-9 < l < 9$
Intensity control				
Decay, corrected	2.3%, no	2.6%, no	2.9%, yes	3.9%, no[b]
Refl. measured	2428	2927	6138	2028
Unique refl.	730	939	1657	1091
R_{int} (all)	0.031	0.016	0.054	0.038
Extinction coef.	0.070(7)	0.027(2)	—	0.121(6)
Absorption			ABSORB[c]	ABSORB[c]
μ/mm^{-1}	1.18	1.00	5.65	4.39
T_{min}, T_{max}	—	—	0.336, 0.891	0.315, 0.692
Refinement	F^2	F^2	F^2	F^2
Refl. refined	730	939	1657	1087[d]
Refl. observed	676	859	1280	1029
Conditions	$F_o > 4\sigma(F_o)$	$F_o > 4\sigma(F_o)$	$F_o > 4\sigma(F_o)$	$F_o > 4(F_o)$
Parameters	65	80	127	80
Final R, wR[e]	0.037, 0.099	0.029, 0.076	0.035, 0.071	0.030, 0.095
Residual density	0.35, −0.20	0.22, −0.16	0.47, −0.57	0.33, −0.26
S	1.102	1.048	0.722	1.279
Weighting param.[f] par1, par2	0.0571, 0.0594	0.0341, 0.1475	0.0, 0.0	0.0068, 0.0067

[a] Data were collected at 122 K. [b] Variation in control reflections. [c] De Titta (1985).[10] [d] Four reflections omitted during refinements due to systematic errors. [e] Based on all unique reflections. [f] Weighting scheme: $w = 1/[\sigma^2(F_o^2) + (\text{par1 } P)^2 + \text{par2 } P]$; $P = [\max(F_o^2, 0) + 2F_c^2]/3$.

were measured using NMR spectroscopy, and their possible importance for the receptor affinity is discussed.

Results

X-Ray crystallography

A summary of the crystal data and structure determinations of **3**–**6** is given in Table 1. Selected structural parameters are shown in Table 2. The geometries of **3** and **5** are comparable to earlier observations for nonionized isoxazol-3-ols,[11] whereas there are only scarce literature data for comparison with the structures of **4** and **6**. Thus, a search of the Cambridge Structural Database [12] for compounds containing the isothiazol-3-ol moiety resulted in five hits (AEBZTZ,[13] EABZIT,[14] HMSPTZ,[15] JIGCIL [16] and YEMLOR [17]), only one (HMSPTZ) containing the free 3-hydroxy group in a substituted isothiazole ring. Substitution of sulfur for oxygen in the heterocyclic ring (**3**→**4** and **5**→**6**) has little effect on the ring geometry, except for that imposed by the larger covalent radius of the sulfur atom. Thus, the bonds to sulfur are longer than the corresponding bonds to oxygen by 0.25 Å for X(1)–N(2) and 0.35 Å for X(1)–C(5) (Table 2). The C(4)–C(5) bonds show a slight elongation (*ca.* 0.01–0.02 Å) in the isothiazol-3-ols. The bond angles within the ring expand to accommodate the larger sulfur atom, except for the C(4)–C(5)–X(1) angle which is slightly contracted, and the angle centred at the sulfur atom, which is 94–95° in **4** and **6** as compared to *ca.* 108° for the corresponding oxygen-centered angle in **3** and **5**. Upon substitution of sulfur for oxygen, the van der Waals volume (determined using SYBYL[18]) of the heterocyclic ring increases from 61.6 to 70.2 Å^3. The distance between N(2) and the hydroxylic oxygen in **3**–**6** is in the range 2.318–2.322 Å.

The distortions observed upon introduction of the methyl group at C(5) (**3**→**5** and **4**→**6**) are almost negligible (Table 2). The small changes that are observed can be explained as due mainly to repulsion between the methyl group and the ring heteroatom. The bond C(5)–X(1) is longer in the methyl substituted compounds (*ca.* 0.01 Å) and the ring angle centred at C(5) is compressed by *ca.* 1°. The crystal packings of all four compounds show dimers of molecules (Figs. 1 and 2),[19] with hydrogen bonds between O(3)–H and N(2). Dimerization occurs around an inversion centre. Geometries of the H-bonds in the dimers are comparable (Table 3), but not identical. Thus, the O–H bonds are shorter and the H · · · N distances longer in the isothiazol-3-ols than in the isoxazol-3-ols.

All compounds show stacks of the heterocyclic rings, but with different packing of these stacks (Fig. 2). The rings of isoxazol-3-ol **3** show a stacking direction almost perpendicular to the plane of the ring. Successive rings form hydrogen bonds to neighbouring stacks on the opposite sides. Hydrogen bonding between the stacks thus creates a two-dimensional network. Neighbouring stacks are slightly displaced, so that the interplanar distance between the two rings in a dimer is 0.55 Å, to allow back-edges [C(4)–C(5)] of the successive dimers to interleave.

In isothiazol-3-ol **4**, the hydrogen bonds are always formed

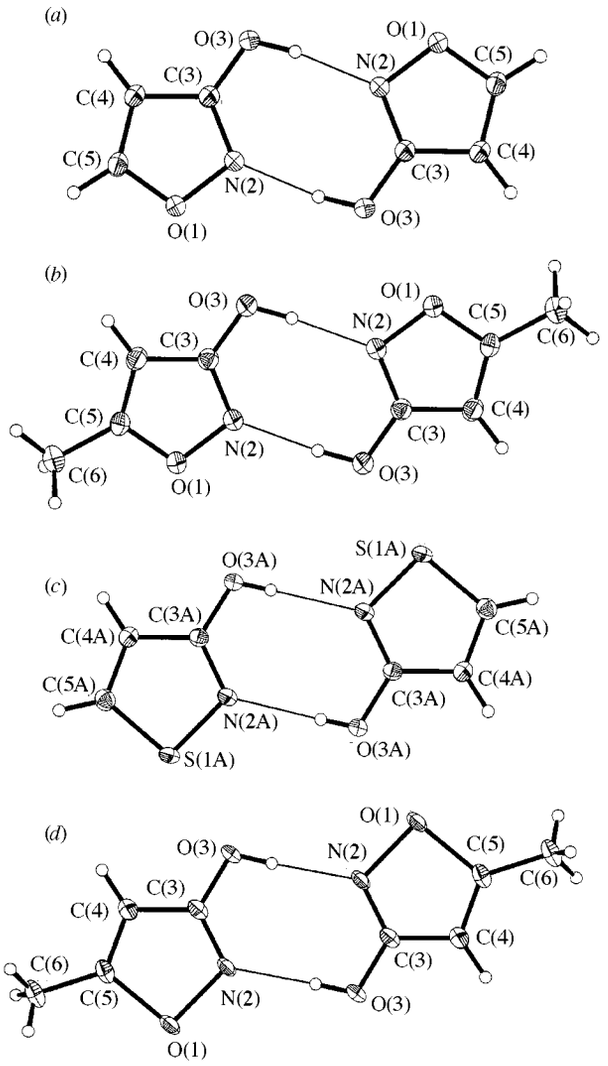

Fig. 1 Molecular structures of the dimers observed in the crystals of **3** (*a*), **5** (*b*), **4** (*c*) and **6** (*d*) (ORTEPII[19]). Atomic labelling and displacement ellipsoids at the 50% probability level are shown for non-hydrogen atoms. Hydrogen bonds are illustrated as thin lines.

between the same neighbouring stacks, so that the crystal packing shows stacks of almost planar dimers (interplanar distances of only 0.16 and 0.19 Å for the symmetry-independent dimers). However, the dimers are strongly tilted, resulting in a fishbone-like packing. Neighbouring stacks of dimers are packed with angles between the planes of dimers of *ca.* 80°, thus enabling favourable edge-to-face interactions of the dimers similar to that observed in benzene (the crystal structure of benzene shows successive T-shaped edge–face interactions[20]).

The crystal packing of **5** shows the same tilted stacks of dimers as observed for **4**, also with an interplanar angle of *ca.* 80° between the neighbouring dimers. However, the methyl substituent precludes the favourable edge–face interactions in this case.

The dimers of **6** are completely planar. As in the structure of **3**, a two-dimensional network is created by alternation of hydrogen bonds to stacks on opposite sides. The presence of the methyl group precludes the interleaving of back-edges of successive dimers as observed with **3**. However, the displacement of neighbouring stacks still causes the heterocyclic rings to tilt strongly with respect to the stacking direction.

Acidity constants

^{13}C NMR titrations of **3** and **4** gave monophasic titration curves defined by eqn. (1), where δ_i is the observed chemical

$$\delta_i = (\delta_i^{1}[H^+] + K_a\delta_i^{0})/(K_a + [H^+]) \quad (1)$$

shift of the *i*-th carbon at any pH, δ_i^{0} and δ_i^{1} are the chemical shifts of the *i*-th carbon in the nonprotonated and monoprotonated species, and K_a is the acid–base equilibrium constant.

The NMR titrations were performed at a relatively high salt concentration (1.0 M) to maintain constant ionic strength during the experiment. Except for C(5), all carbon atoms experienced a downfield shift with increasing pH. The largest ionization shift ($\Delta\delta$ *ca.* 7 ppm) was observed for C(3), directly attached to the hydroxy group. Nonlinear fitting of the NMR titration curve [eqn. (1)] to the experimental data yielded the intrinsic chemical shift data (δ_i^{n}) and the pK_a values[21] of 5.85 and 7.54 for **3** and **4**, respectively. The molar fractions of the anionic forms at the physiological pH = 7.4, calculated from eqn. (2), are 0.97 and 0.42 for **3** and **4**, respectively.

$$x_a = 1/(1 + 10^{pK_a - pH}) \quad (2)$$

Ab initio calculations

Bond lengths and angles optimized for **3**–**6** at the HF/6-31G* level, as well as at the MP2/6-311G** level for **3** and **4**, are shown in Table 2. In order to gain insight into the structural changes upon dimerization, the calculations were also performed on the complex **15** as a model for the dimer of **3**. The

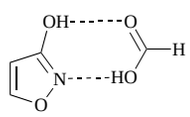

15

complex was subjected to optimization and normal mode analysis at the HF/6-31G* level in C_s symmetry. Hydrogen bonds are less well modelled than covalent bonds at the HF/6-31G* level, but they are still expected to be reasonably accurate.[22] It is hence expected that changes in the geometry of the ring upon hydrogen bonding will show the correct trend if not the absolute values with this basis set. The rms deviations of bond lengths and angles between the X-ray structures and the calculated geometries are shown in Table 4. The calculated dipoles and partial charges of the four molecules are shown in Fig. 3. A superposition of the molecules **3**–**6** and **15**, as calculated at the HF/6-31G* level, is shown in Fig. 4.

In agreement with the observations in the crystal studies, the structural changes in the ring upon substitution in the 5-position (**3**→**5** and **4**→**6**) are almost negligible. In the isothiazol-3-ol series, the S(1)–C(5) bond is elongated by *ca.* 0.01 Å due to repulsion between the methyl group and the sulfur atom. The methyl group also causes a small increase in the overall polarity of the system. The electrostatic potential (ESP) derived charges indicate a small electron shift from C(5) to C(4) upon methyl substitution (Fig. 3).

The most significant electronic effect upon the substitution of sulfur for oxygen in the heterocyclic rings is observed for the C(4)–C(5) bond. In the isoxazol-3-ols, this bond is strongly polarized due to a σ-withdrawal of charge from C(5) to O(1) in conjunction with π-donation from O(1) to C(4). The sulfur atom is much less electronegative than the oxygen atom, and is also a poor π-donor, which leads to strong depolarization of the C(4)–C(5) bond in the isothiazol-3-ols compared to isoxazol-3-ols. The low electronegativity also leads to a small, positive net charge on the sulfur atom (Fig. 3).

Geometry optimization of the complex **15** shows that the effect of hydrogen bonding on the ring geometry is small. An overlap of all heavy atoms in **3** with the corresponding atoms in **15** gave rms deviation of only 0.008 Å. As expected, the electrons of the hydroxylic oxygen become more available for conjugation, and a slight compression of the C(3)–O(3) bond and an even smaller elongation of the N(2)–C(3) bond (*ca.* 0.01 Å) are observed. The N(2)–C(3)–O(3) angle is expanded by *ca.* 1°.

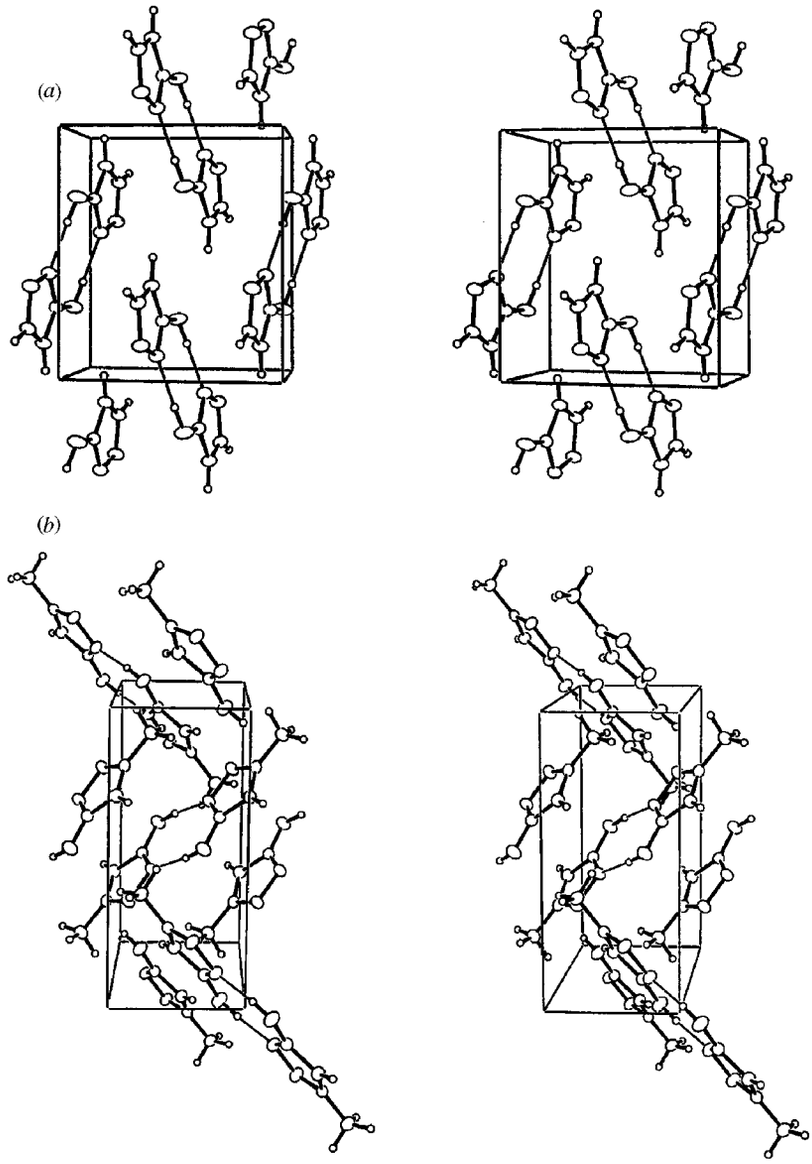

Fig. 2 Crystal packings of the four compounds analysed (*a*) **3**, *c*-axis horizontal, *b*-axis vertical and *a*-axis into plane of paper; (*b*) **5**, *a*-axis horizontal, *b*-axis vertical and *c*-axis out of plane of paper; (*c*) **4**, *b*-axis horizontal, *a*-axis vertical and *c*-axis into plane of paper; (*d*) **6**, *b*-axis horizontal, *a*-axis vertical and *c*-axis into plane of paper

For **3** and **4**, the main effect of the increase of the computational level from HF/6-31G* to MP2/6-311G** is to elongate most bonds, except for C(3)–C(4) which is shortened by 0.007 Å in **3** and 0.017 Å in **4** (Table 2). The two bonds to sulfur atoms are also slightly shorter in the high-level geometries. The largest elongation (*ca*. 0.04 Å) is seen for N(2)–C(3), but all carbon–oxygen bonds, as well as C(4)–C(5) bond in both molecules are also stretched by at least 0.02 Å. As expected, the correlated calculations result in generally less pronounced charges and smaller dipole moments (Fig. 3).

Discussion

The structural features of the O(3)–C(3)–N(2) fragment of isoxazol-3-ols and isothiazol-3-ols correspond well to those of the O–C–O carboxylic acid moiety which they replace in the bioisosteric analogues. Data for nonionized carboxylic acids (1993 observations, $R \leqslant 0.06$) have been retrieved from the Cambridge Structural Database.[12] The central angle, 118–128° in the carboxylic acids (mean 123.5°), is 122.0–122.7° in **3**-**6** (Fig. 5). The distance from O(3) to N(2), 2.318–2.322 Å in **3**–**6**, is only slightly longer compared to the range found for the O···O distance in the carboxylic acids (2.16–2.24 Å, mean 2.220 Å) (Fig. 5). The isoxazol-3-ols as well as isothiazol-3-ols, such as **7**–**14**, are thus expected to be well suited for binding to receptor sites with primary interatomic interactions similar to those in the corresponding carboxylic acids **1** and **2**.

For binding of various carboxylic acid bioisosteres to specific receptors, changes of affinity are expected to be correlated with the steric bulk, electronic complementarity, strength of the primary interaction and geometry of spacer units in cases of multiple interactions. These factors are considered in order below.

Within a constrained binding environment, excess volume occupied by the ligand could have a severe detrimental effect on the binding. As shown in Fig. 4, it is possible to overlap the carboxy-bioisosteric moieties of the heterocycles [N(2), C(3), (O3), C(4)] with very good correspondence. The largest rms deviation of the four-atom overlap is 0.04 Å. S(1) and C(5) are displaced away from the N(2)–C(3)[O(3)]–C(4) fragment compared to O(1) and C(5) in the isoxazol-3-ols. A crowded binding environment could therefore disfavour the isothiazol-3-ols selectively, although the difference in the volumes is small (15%). However, since the heterocycle-containing analogues show high affinity to the receptors which have carboxylic acids as the native ligands, the receptors can apparently accom-

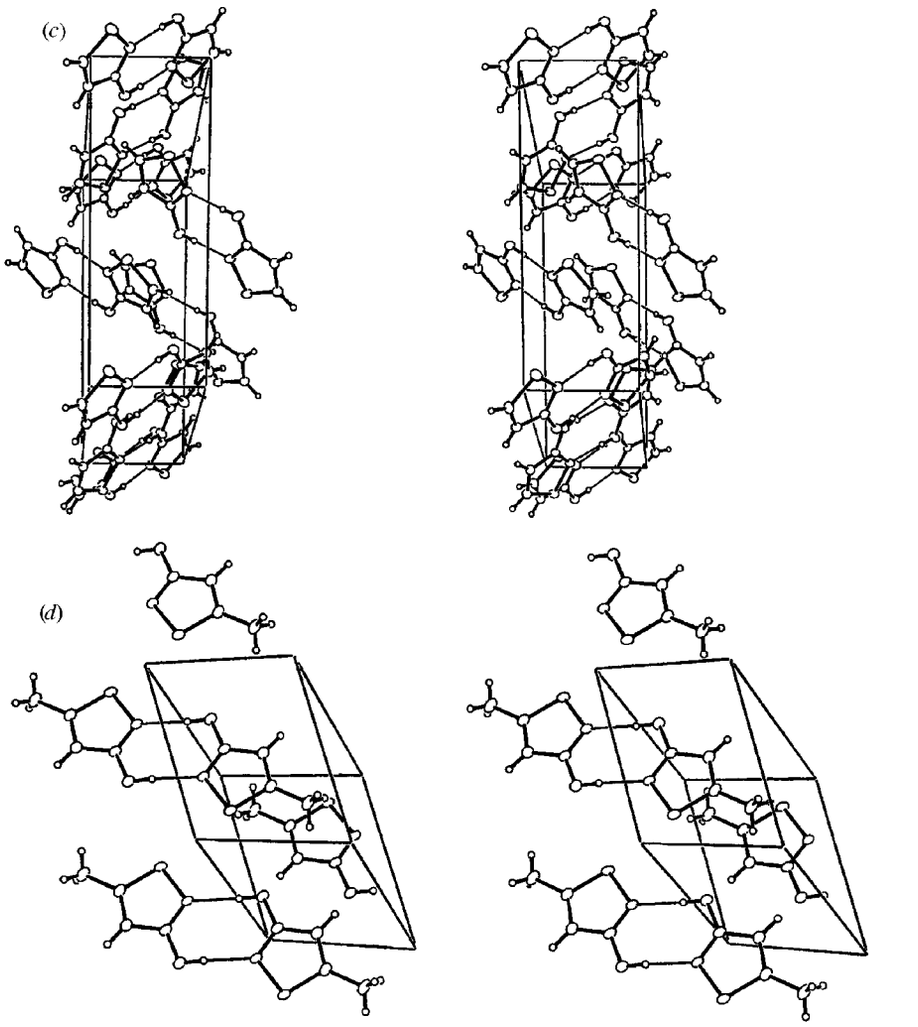

Fig. 2 (*continued*)

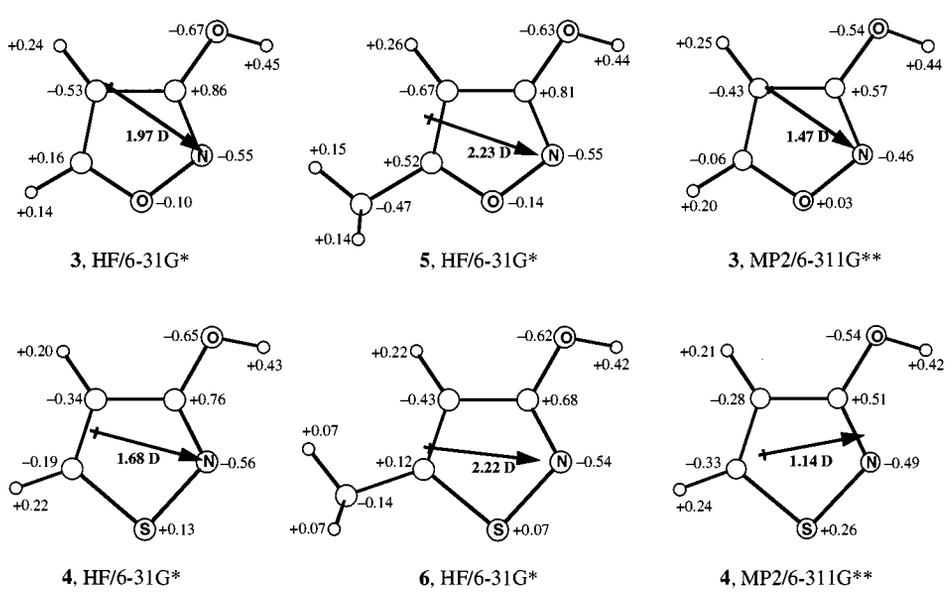

Fig. 3 Calculated dipole moments and ESP (CHELPG) charges in **3**–**6**

modate the steric bulk associated with the heterocyclic rings, and the steric differences at position 1 of the ring are unlikely to modulate the affinity to any great extent.

The relative geometry of pharmacophore elements in a ligand may also be affected by the substitution of isothiazol-3-ols for isoxazol-3-ols. The least-square fits show that this effect is largest for the substituents in the 5-position of the heterocyclic ring (Fig. 4). The distance from N(2) to C(6) [carbon atom connected to C(5)] increases by 0.36 Å when going from **5** to **6**. The same magnitude of increase (0.33 Å) is noted for the N(2)···H(5) distance in the unsubstituted compounds **3** and **4**. The effect is much smaller at the 4-position, the N(2)···H(4) distance being increased only by *ca*. 0.04 Å when going from isoxazol-3-ols to isothiazol-3-ols. Thus, the effect of exchange

Table 2 Experimental (X-ray) and calculated (*ab initio*) bond lengths (Å) and bond angles (°)

	3			**15**	**5**	
	X-Ray	HF/6-31G*	MP2/6-311G**	HF/6-31G*	X-Ray	HF/6-31G*
O(1)–N(2)	1.410(1)	1.372	1.380	1.373	1.417(1)	1.376
N(2)–C(3)	1.312(1)	1.282	1.321	1.290	1.312(1)	1.281
C(3)–C(4)	1.421(2)	1.427	1.420	1.429	1.418(1)	1.425
C(3)–O(3)	1.332(1)	1.326	1.346	1.310	1.330(1)	1.327
C(4)–C(5)	1.341(2)	1.339	1.364	1.337	1.343(2)	1.343
C(5)–O(1)	1.350(1)	1.319	1.347	1.319	1.360(1)	1.323
C(5)–C(6)					1.482(2)	1.490
C(5)–O(1)–N(2)	107.67(8)	109.14	109.05	108.70	108.07(8)	109.75
O(1)–N(2)–C(3)	105.44(9)	105.38	105.39	106.12	105.21(8)	105.05
N(2)–C(3)–C(4)	112.1(1)	112.57	112.46	111.51	112.1(1)	112.67
N(2)–C(3)–O(3)	122.45(9)	122.68	121.96	123.86	122.7(1)	122.53
C(4)–C(3)–O(3)	125.5(1)	124.75	125.59	124.64	125.3(1)	124.81
C(3)–C(4)–C(5)	103.5(1)	101.65	102.46	102.24	104.5(1)	102.27
C(4)–C(5)–O(1)	111.3(1)	111.26	110.65	111.44	110.2(1)	110.27
C(4)–C(5)–C(6)					133.6(1)	132.99
O(1)–C(5)–C(6)					116.2(1)	116.74

	4				**6**	
	X-Ray[a]		HF/6-31G*	MP2/6-311G**	X-Ray	HF/6-31G*
S(1)–N(2)	1.666(2)	1.666(2)	1.665	1.660	1.670(1)	1.669
N(2)–C(3)	1.320(2)	1.319(2)	1.279	1.323	1.317(2)	1.278
C(3)–C(4)	1.421(2)	1.426(2)	1.439	1.422	1.429(2)	1.438
C(3)–O(3)	1.334(2)	1.332(2)	1.331	1.352	1.334(2)	1.331
C(4)–C(5)	1.354(2)	1.357(3)	1.342	1.376	1.361(2)	1.344
C(5)–S(1)	1.697(2)	1.701(2)	1.718	1.708	1.709(2)	1.730
C(5)–C(6)					1.499(2)	1.500
C(5)–S(1)–N(2)	94.59(9)	94.32(9)	93.72	95.14	95.07(7)	94.27
S(1)–N(2)–C(3)	109.1(1)	109.4(1)	109.58	108.66	108.9(1)	109.16
N(2)–C(3)–C(4)	116.0(2)	116.1(2)	117.53	117.40	116.4(1)	117.73
N(2)–C(3)–O(3)	122.1(2)	122.2(2)	122.13	120.88	122.0(1)	122.03
C(4)–C(3)–O(3)	121.9(2)	121.7(2)	120.34	121.73	121.6(1)	120.24
C(3)–C(4)–C(5)	110.3(2)	109.8(2)	108.93	109.22	110.5(1)	109.84
C(4)–C(5)–S(1)	110.0(1)	110.4(1)	110.25	109.59	109.2(1)	109.00
C(4)–C(5)–C(6)					128.6(2)	128.45
S(1)–C(5)–C(6)					122.3(1)	122.56

[a] Two sets of numbers correspond to two molecules present in the asymmetric unit of the cell.

Table 3 Hydrogen bond geometries in **3**–**6** determined by X-ray crystallography

D–H · · · A	D–H/Å	D · · · A/Å	H · · · A/Å	D–H–A/°	Symmetry
3 O(3)–H(3) · · · N(2)	0.92(2)	2.710(1)	1.79(2)	171(2)	$1-x, 1-y, -z$
5 O(3)–H(3) · · · N(2)	0.93(2)	2.721(1)	1.80(2)	175(2)	$-x, -y, -z$
4 O(3)–H(3) · · · N(2)[a]	0.77(2)	2.735(2)	1.96(3)	177(3)	$2-x, 1-y, 1-z$
	0.86(3)	2.706(2)	1.85(3)	177(3)	$1-x, 2-y, 1-z$
6 O(3)–H(3) · · · N(2)	0.86(2)	2.720(2)	1.86(2)	177(2)	$1-x, -y, -z$

[a] Two molecules present in the asymmetric unit of the cell.

of the heteroatom at the 1-position and that of the 5-substituent may be expected to show synergy, whereas changes at the 4-position should have similar effect in both series of the heterocycles (assuming identical binding mode). Electronically, the nonionized heterocyclic units are similar. It is also hard to predict which electronic features will be of importance in the absence of exact knowledge about the structure of the receptor site. The dipoles of the two systems are very similar, particularly in the 5-methylated species (**5** and **6**) (Fig. 3).

The heterocyclic systems under consideration are bioisosteres of carboxylic acids. It is therefore reasonable to assume that one of the primary binding interactions with the receptor will be a strong interaction between a hydrogen bond donor in the receptor and the anion of the carboxylic acid analogue, and that the acidity of the analogue will play a central role. The NMR titrations showed that the isothiazol-3-ol **4** is 1.7 pK_a unit less acidic than the isoxazol-3-ol **3**, and this difference is expected to persist for all derivatives except those containing strongly electronegative substituents.[9,23] In terms of acidity, isoxazol-3-ols are thus more reminiscent of carboxylic acids than isothiazol-3-ols.

In order to describe the relative efficiency of the interaction between the heterocyclic unit and the binding site, we consider the two equilibria shown in reactions (3) and (4).

Reaction (3) describes the protonation of the anion, the equilibrium constant of which is the reciprocal of the acidity constant K_a. Reaction (4) is a model for the interaction of the anion with one functional group (FG) at the receptor site. At this stage, we neglect other possible interactions with the remaining part of the binding site. All species in reactions (3) and (4) are hydrated, but we consider only the differences in the equilibrium free energies and therefore assume that the contributions from solvation can be neglected. We postulate a linear relationship between the free energies of equilibria (3) and (4), *i.e.* $\ln K_b = \text{constant} \times \ln(K_a^{-1})$.

The equilibrium free energy of reaction (3) is, by definition, given by eqn. (5). The total affinity K_{aff} of the heterocyclic unit

Table 4 Comparison between structure determination methods. Deviations are calculated from bonds and angles including non-hydrogen atoms only.

Comparison	Structure(s)	Rms bond deviation/Å	Rms angle deviation/°
HF/6-31G* *vs.* X-ray	**3**	0.024	0.96
	4[a]	0.020	0.95
	5	0.024	1.00
	6	0.018	0.74
	15	0.024	0.94
HF/6-31G*, structure differences[b]	**3** *vs.* **5**	0.003	0.52
	4 *vs.* **6**	0.005	0.65
	3 *vs.* **15**	0.007	0.72
MP2/6-311G** *vs.* HF/6-31G*	**3**	0.024	0.57
	4	0.026	0.99
MP2/6-311G** *vs.* X-ray	**3**	0.017	0.74
	4[a]	0.012	0.89
'MP2 + H-bond'[c] *vs.* X-ray	**3**	0.016	0.62
	4[a]	0.010	0.30

[a] Average of data for independent units in the crystal. [b] Comparisons include only non-hydrogen atoms in **3** and **4**, respectively. [c] Calculated by adding the differences between the HF/6-31G*-structures of **3** and **15** to the MP2/6-311G** structures.

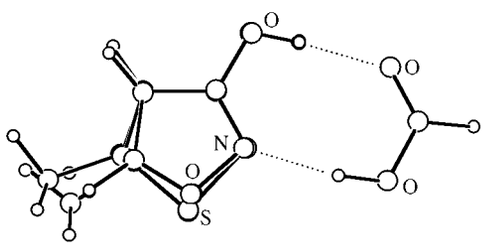

Fig. 4 Superposition of the molecules of **3**–**6** and **15**, as calculated at the HF/6-31G* level. The atoms fitted were N(2), C(3), O(3) and C(4). The rms deviations are in all cases <0.04 Å.

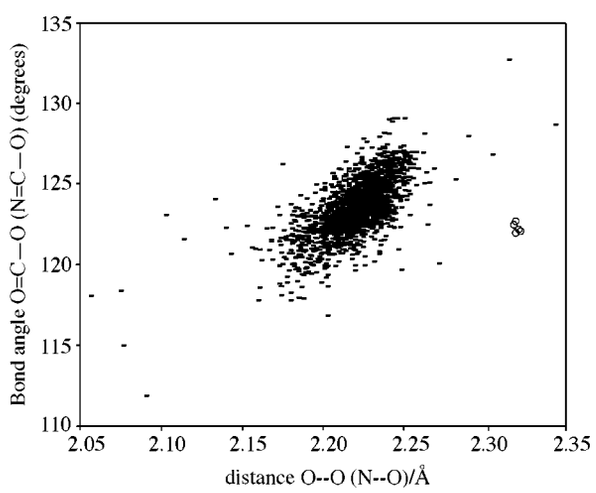

Fig. 5 Scatter plot showing the range of experimental values adopted by O · · · O distances and O–C–O bond angles in nonionized carboxylic acids (-), with the corresponding N–C–O dimensions in the X-ray structures of **3**–**6** (○)

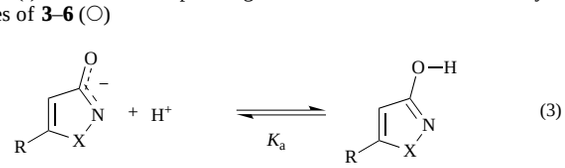

(3)

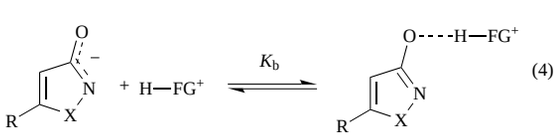

(4)

$$\Delta G_a = RT \ln K_a = -pK_a RT \ln 10 \quad (5)$$

for the receptor functional group (FG) can be considered to be the product of the molar fraction of the compound present in the anionic form [x_a, reaction (2)] and the binding equilibrium constant K_b [reaction (4)]. To estimate the affinity K_{aff}, we must find a description for K_b. One way of expressing the free energy relationship between the reactions (3) and (4) is shown in eqn. (6). Here, ln*c*/ln10 is the proportionality constant between pK_a and pK_b. We now obtain the relationship shown in eqn. (7).

$$\Delta G_b = -RT \ln K_b = -pK_a RT \ln c,\ c > 1 \quad (6)$$

$$K_{aff} = x_a K_b = c^{pK_a}/(1 + 10^{pK_a - pH}) \quad (7)$$

It can easily be demonstrated that as long as $1 < c < 10$, eqn. (7) will show a maximum for heterocycles with a pK_a similar to the pH. In the family of $GABA_A$ agonists and antagonists, the highest affinities are always obtained for compounds with pK_a in the range 4–6.[5] A value of $c \approx 1.3$ gives a predicted affinity maximum approximately one pK_a unit below the pH, with the observed sharp cutoff in activity above the maximum and a smooth decrease below. Although the exact nature of the postulated linear free energy relationship between reactions (3) and (4) has yet to be elucidated, the available biological data show that the isoxazol-3-ols generally show a higher activity than isothiazol-3-ols.[3,9] A notable exception is the pair **13** and **14,** for which the reverse relationship was found.[9] However, the bulky *tert*-butyl substituent present in this case may cause special steric effects, causing **14** to relocate relative to **13** in the binding site, leading to altered interactions and modulation of activity in an atypical way.

It appears that the difference in the acidity is the primary factor affecting the activity of isoxazol-3-ols and isothiazol-3-ols, possibly *via* a relationship similar to eqn. (7). The steric and geometrical effects of sulfur alone, or alteration of electronic properties such as dipole moments, appear to be too small to account for the differences in receptor affinity, which for AMPA (**11**) and its sulfur analogue **12** amounts to a factor of 45.[9] A detailed analysis of the charge distribution in ionized isoxazol-3-ols and isothiazol-3-ols has yet to be carried out.

The present study allowed a detailed comparison between the experimental X-ray geometries of the isoxazol-3-ols and the isothiazol-3-ols with the *ab initio* geometries, which helps to assess the usefulness of the computational level used for prediction of geometries of bioisosteric neurotransmitter analogues. In the X-ray structures, strong intermolecular hydrogen bonds are observed, and they are expected to alter the geometries of the rings. Comparisons of the HF/6-31G* results with the results of the X-ray structure determinations (Tables 2 and 4) show rms deviations for all compounds of about 0.02 Å for bonds and 1° for angles. Thus, the HF/6-31G* level, which has become a standard for production level work,[24] is indeed accurate enough for routine predictions. However, the geometrical differences are still substantially larger than standard errors from experimental determinations. For tasks where the need for accurate data is stronger, as in the determination of general force field parameters,[24] higher levels of theory must be applied. The systems under investigation contain close contacts between mobile electrons, especially between lone pairs of nitrogen and oxygen, but also between the lone pair electrons and π-systems. The description of the system would therefore be expected to be improved by the inclusion of electron correlation treatment.

The effects of intermolecular hydrogen bonding were investigated at the HF/6-31G* level using formic acid as a model of the second component of the dimer. This model is not expected to be perfect since formic acid is more acidic than **3**, and because the lone pair donating power of carbonyl oxygen of formic acid should be substantially lower than that of N(2) in isoxazole, but the structural changes are expected to show correct trends (Tables 2 and 4). All significant changes centre around the N(2)–C(3)–O(3) moiety, as expected from chemical

intuition. The hydrogen bonding will release some electron density to O(3) and remove some from N(2), thereby increasing conjugation in the C(3)–O(3) bond. As a result, C(3)–O(3) is shortened, N(2)–C(3) is slightly elongated in the complex, and the N(2)–C(3)–O(3) angle is expanded by *ca.* 1°. The changes are small and the overall improvement in geometry compared to the geometry of **3** observed in crystals is negligible.

The largest differences in bond length prediction at the HF/6-31G* level are found for the O(1)–N(2) bond in the isoxazol-3-ols (*ca*. 0.04 Å), closely followed by the N(2)–C(3) bond in all molecules (0.03–0.04 Å). The O(1)–N(2) bond is reminiscent of a peroxide bond, which is known to be very difficult to describe computationally.[25] The two simplest molecules (**3** and **4**) have therefore been reoptimized at the MP2/6-311G** level. It can be seen (Tables 2 and 4) that most bonds are elongated significantly, and the bond length rms deviation is lowered to 0.017 Å for **3** and to 0.012–0.013 Å for **4**, resulting in improved description of the structure, especially when HF/6-31G* corrections for hydrogen bond effects are added (Table 4). A corollary of this is that the geometries at the MP2 level of calculations are expected to represent the gas phase geometries of **3** and **4** well. This computational level therefore seems sufficient for a force field parametrization, the first step in a more accurate description of the ligand–receptor interaction.

Experimental

X-Ray crystallographic analysis

Isoxazol-3-ol (**3**),[26] isothiazol-3-ol (**4**)[27] and 5-methylisothiazol-3-ol (**6**)[21] were synthesized as previously described; 5-methylisoxazol-3-ol (**5**) was obtained from Sankyo Co., Ltd. (Tokyo). Single crystals were obtained from solutions in light petroleum. One crystal was used for the determination of the unit cell parameters and for the collection of intensity data (ω–2θ scan mode); θ-limit for all compounds was 75°. The measurements were performed at 122 ± 0.5 K on an Enraf-Nonius CAD-4 diffractometer. The crystals were cooled in a stream of nitrogen gas provided by an Enraf-Nonius low-temperature device. Data reduction was performed with the program DREADD.[28] The positions of the non-hydrogen atoms were obtained by application of direct methods (SHELXS86[29]). The hydrogen atoms were subsequently located on a series of difference electron density maps. Final full-matrix least-squares refinements (SHELXL93[30]) included an overall scale factor, an extinction parameter (except for **4**), atomic coordinates for all atoms, and anisotropic displacement parameters for non-hydrogen atoms. The isotropic displacement parameters for the hydrogen atoms were fixed. The quantity minimized was $\Sigma w(|F_o^2| - k|F_c^2|)^2$. Atomic scattering factors used are those found in International Tables[31] and included in SHELXL93. A summary of structure determination details and crystal data is given in Table 1. Atomic coordinates, bond lengths and angles, and thermal parameters have been deposited at the Cambridge Crystallographic Data Centre (CCDC). See Instruction for Authors, *J. Chem. Soc., Perkin Trans. 2*, 1997, Issue 1. Any request to the CCDC for this material should quote the full literature citation and the reference number 188/77.

Searches in the Cambridge Structural Database were performed using ver. April 1996.[12]

NMR spectroscopy

A solution of **3**[26] (10 mg, 0.1 mmol) and **4**[27] (20 mg, 0.2 mmol) in 0.6 ml H_2O–D_2O (9:1), 1 M in KCl, was made alkaline with 1 M NaOH. The solution was titrated with 0.5 M HCl adjusted to the ionic strength of 1 M with KCl; the pH was measured directly in the NMR tubes, before and after acquiring the ^{13}C NMR spectrum, using a glass microelectrode. Since the carbon resonances of **3** and **4** were well resolved, both heterocycles could be titrated simultaneously, which made the pK_a difference obtained independent of errors in pH readings. The $^{13}C\{^1H\}$ NMR spectra were recorded at 25 °C with a Bruker AMX 400 WB spectrometer operating at 100.62 MHz for ^{13}C. The spectra were standardized to internal 3-(trimethylsilyl)-propanesulfonate. The nonlinear curve fitting was carried out with Ultrafit ver. 2.11 program from Biosoft, Cambridge, UK, using a Levenberg–Marquardt algorithm. The following ionization shifts ($\Delta\delta = \delta_{base} - \delta_{acid}$) were observed: **3**, C(3) 7.10, C(4) 2.65, C(5) −1.39; **4**, C(3) 6.65, C(4) 2.13, C(5) −0.32.

Computations

Ab initio optimizations of the structures **3–6** were performed at the HF/6-31G* level, in either Spartan[32] or Gaussian 94.[33] Geometries were optimized with C_s symmetry and characterized as minima by normal mode analysis. Geometries of **3** and **4** were also optimized at the MP2/6-311G** level. ESP (CHELPG) charges were determined in Spartan.[32]

Acknowledgements

This work was supported by the Lundbeck Foundation, the Alfred Benzon Foundation, the Danish State Biotechnology Programme (1991–1995) and the Danish Medical Research Council. The assistance of Mr Flemming Hansen in the collection of X-ray crystallographic data is gratefully acknowledged. 5-Methylisoxazol-3-ol was kindly donated by the company Sankyo Co., Ltd. (Tokyo).

References

1 P. Krogsgaard-Larsen, *Med. Res. Rev.*, 1988, **8**, 27.
2 J. J. Hansen and P. Krogsgaard-Larsen, *Med. Res. Rev.*, 1990, **10**, 55.
3 P. Krogsgaard-Larsen, G. A. R. Johnston, D. R. Curtis, C. J. A. Game and R. M. McCulloch, *J. Neurochem.*, 1975, **25**, 803.
4 P. Krogsgaard-Larsen, G. A. R. Johnston, D. Lodge and D. R. Curtis, *Nature*, 1977, **268**, 53.
5 P. Krogsgaard-Larsen, H. Hjeds, D. R. Curtis, D. Lodge and G. A. R. Johnston, *J. Neurochem.*, 1979, **32**, 1717.
6 L. Brehm, B. Ebert, U. Kristiansen, K. A. Wafford, J. A. Kemp and P. Krogsgaard-Larsen, *Eur. J. Med. Chem.*, 1997, **32**, 357.
7 P. Krogsgaard-Larsen, T. Honoré, J. J. Hansen, D. R. Curtis and D. Lodge, *Nature*, 1980, **284**, 64.
8 J. Lauridsen, T. Honoré and P. Krogsgaard-Larsen, *J. Med. Chem.*, 1985, **28**, 668.
9 L. Matzen, A. Engesgaard, B. Ebert, M. Didriksen, B. Frølund, P. Krogsgaard-Larsen and J. W. Jaroszewski, *J. Med. Chem.*, 1997, **40**, 520.
10 G. T. De Titta, *J. Appl. Crystallogr.*, 1985, **18**, 75.
11 K. Frydenvang, L. M. Hansen and B. Jensen, *Acta Crystallogr., Sect. C*, 1995, **51**, 2053.
12 F. H. Allen and O. Kennard, *Chem. Des. Automation News*, 1993, **8**, 31.
13 A. C. Bonamartini, M. Nardelli, C. Palmieri and C. Pelizzi, *Acta Crystallogr., Sect. B*, 1971, **27**, 1775.
14 A. C. Bonamartini, M. Nardelli and C. Palmieri, *Acta Crystallogr., Sect. B*, 1972, **28**, 1207.
15 J. L. McVicars, M. F. Mackay and M. Davies, *J. Chem. Soc., Perkin Trans. 2*, 1977, 1332.
16 C. B. Vicentini, A. C. Veronese, T. Poli, M. Guarneri, P. Giori and V. Feretti, *J. Heterocycl. Chem.*, 1990, **27**, 1481.
17 K. Stratmann, J. Belli, C. M. Jensen, R. E. Moore and G. M. L. Patterson, *J. Org. Chem.*, 1994, **59**, 6279.
18 SYBYL ver. 6.2. Tripos Associates Inc., St. Louis, Missouri 63144, USA.
19 C. K. Johnson, ORTEPII. Report ORNL-5138. Oak Ridge National Laboratory, Tennessee, USA, 1976.
20 E. G. Cox, D. W. J. Cruickshank and J. A. S. Smith, *Proc. R. Soc. London*, 1958, **247**, 1; R. W. G. Wyckoff, *Crystal Structures, The Structure of Benzene Derivatives*, Interscience, New York, 1969, vol. 6.
21 J. Goerdeler and W. Mittler, *Chem. Ber.*, 1963, 861.
22 S. Scheiner, *Rev. Comp. Chem.*, 1985, **2**, 165.
23 R. Slack and K. R. H. Woolbridge, *Adv. Heterocycl. Chem.*, 1965, **4**, 107; A. Braibanti and M. T. L. Mangia, *Gazz. Chim. Ital.*, 1981, **111**, 71.
24 T. Halgren, *J. Comput. Chem.*, 1996, **17**, 490.
25 W. J. Hehre, L. Radom, P. v. R. Schleyer and J. A. Pople, *Ab initio Molecular Orbital Theory*, Wiley, New York, 1985.

26 I. Iwai and N. Nakamura, *Chem. Pharm. Bull.*, 1966, **14**, 1277.
27 S. N. Lewis, G. A. Miller, M. Hausmann and E. C. Szamborski, *J. Heterocycl. Chem.*, 1971, **8**, 571.
28 R. H. Blessing, *Crystallogr. Rev.*, 1987, **1**, 3; *J. Appl. Crystallogr.*, 1989, **22**, 396.
29 G. M. Sheldrick, *Acta Crystallogr., Sect. A*, 1990, **46**, 467.
30 G. M. Sheldrick, SHELXL93. Program for the Refinement of Crystal Structures. University of Göttingen, Germany, 1995.
31 *International Tables for Crystallography*, Kluwer Academic Publishers, London, 1993, vol. C, Tables 4.2.6.8 and 6.1.1.4.
32 Spartan SGI version 4.0.3 GL Wavefunction Inc. 18401 von Karman, suite 370, Irvine, CA 92715.
33 Gaussian 94 revision D.1, M. J. Frisch, G. W. Trucks, H. B. Schlegel, P. M. W. Gill, B. G. Johnson, M. A. Robb, J. R. Cheeseman, T. Keith, G. A. Petersson, J. A. Montgomery, K. Raghavachari, M. A. Al-Laham, V. G. Zakrzewski, J. V. Ortiz, J. B. Foresman, J. Cioslowski, B. B. Stefanov, A. Nanayakkara, M. Challacombe, C. Y. Peng, P. Y. Ayala, W. Chen, M. W. Wong, J. L. Andres, E. S. Replogle, R. Gomperts, R. L. Martin, D. J. Fox, J. S. Binkley, D. J. Defrees, J. Baker, J. P. Stewart, M. Head-Gordon, C. Gonzales and J. A. Pople, Gaussian, Inc., Pittsburgh, 1995.

Paper 7/00332C
Received 14*th January* 1997
Accepted 16*th April* 1997